Electronic Supplementary Information

for

3d-4f magnetic exchange interactions and anisotropy in a series of heterobimetallic vanadium(IV)-lanthanide(III) Schiff base complexes

Kamil Kotrle,[a] Ivan Nemec,[a] Jan Moncol,[b] Erik Čižmár,[c] Radovan Herchel *[a]

[a] *Department of Inorganic Chemistry, Faculty of Science, Palacký University, 17. listopadu 12, CZ-771 46 Olomouc, Czech Republic , E-mail: radovan.herchel@upol.cz, www.agch.upol.cz*

[b] *Department of Inorganic Chemistry, Faculty of Chemical and Food Technology, Slovak University of Technology in Bratislava, Bratislava SK-81237, Slovakia*

[c] Institute of Physics, Faculty of Science, P.J. Šafárik University in Košice, Park Angelinum 9, SK-041 54 Košice, Slovakia

Table S1: List of selected published complexes of Cu(II) – Ln(III)

Structure	J (cm^{-1})	τ_0 (s^{-1})	U_{eff} (K)	Ref
[Cu2Tb2L42(NO3)4]	> 0	$1.7\cdot10^{-10}$	32	1
[Cu2Dy2L42(NO3)4]	> 0			1
[CuGd(L5)(NO3)3]	4.38/6.59			2
[DyCuL(CH3COO)2(NO3)]	> 0			3
[CuGd(L6)Cl3(CH3OH)2]	7.78			4
[CuGd(S,S-L7)(NO3)3(CH3OH)]n	12.57			5
[CuGd(R,R-L7)(NO3)3(CH3OH)]n	14.816			5
[CuGd(L8)(CF3SO3)3(H2O)2]	8.0(2)			6
[CuGd(L7)(CF3SO3)2(H2O)2](CF3SO3)·H2O·CH3COCH3	8.6(2)			6
[CuGd(L9)(NO3)2]2	6.94			7
[CuGd(L4)(NO3)2]2	7.26			7
[CuGd(L10)(NO3)2]2	3.94			7
[CuGd(L11)(NO3)2(H2O)]2	2.80			7
[CuGd(L12)(NO3)2(H2O)]2	4.16			7
[CuGd(L13)(NO3)2(H2O)]2	5.89			7
[CuGd(L13)(C7H6NO2)2]2	2.56			7
[CuGd(L7)(NO3)3(H2O]	12.6			8
[CuGd(L14)(NO3)3]	10.8			8
[CuGd(L15)(NO3)3]	8.08			9
[CuGd(L16)(NO3)2.5(OH)0.5(H2O)]·0.5 H2O	3.3			10
[CuGd(L17)(NO3)3]	1.3			10
[CuGd(L18)(CF3COO)3(CH3OH)2]	4.42(1)			11
[CuGd(L19)(NO3)3(CH3COCH3)]	5.6			12
[CuGd(L3)(Cl)2(H2O)4]Cl·2H2O	10.1			13
[CuGd(L3)(Cl)3(H2O)6]	8.8(4)			13
[CuGd(L2)(N3C2)3(H2O)	7.8(1)			13
[CuGd(L2)(CF3COO)3(H2O)	6.3(1)			1313
[CuGd(L20)(NO3)(H2O)3]	11.4			14
[CuGd(L3)(NO3)3(CH3COCH3)]	6.9			15
[CuTb(L3)(NO3)3(CH3COCH3)]	>3.3	$7.1(9)\cdot10^{-10}$	42.3(4)	15
[CuDy(L3)(NO3)3(CH3COCH3)]	1.63(1)	$4(2)\cdot10^{-10}$	11.5(10)	15
[CuHo(L3)(NO3)3(CH3COCH3)]	1.09(2)			15Error! Bookmark not defined.
[CuEr(L3)(NO3)3(CH3COCH3)]	0.24(1)			15
[CuGd(L3)(CH3)3(CH3COCH3)]	5.2			16
[CuGd(L6)(CH3COO)(CF3COCH2COCF3)2]	5.2			17
[CuTb(L3)(MeOH)(NO3)2(sal)]	4.2(2)	$3.0(8)\cdot10^{-8}$	32.9(4)	18
[CuDy(L3)(MeOH)(NO3)2(sal)]	2.0(2)	$1.02(11)\cdot10^{-5}$	26.0(5)	18
[CuHo(L3)(MeOH)(NO3)2(sal)]	1.3(1)			18
[CuGd(L21)(NCS)3(H2O)(CH3COCH3)]	9.20			19
[CuGd(L22)(NCS)3(H2O)]·2(CH3COCH3)	5.5			19
[CuGd(L23)(NO3)2(H2O)3]NO3	5.08			20
[CuTb(L23)$(NO_3)_3$(MeOH)]		$2.1\cdot10^{-8}$	24.6	20

Hsal = salicylaldehyde, for L1 – L23 see Figure S1

Table S2 Crystallographic data for the reported compounds **1**-**4**.

	1	**2**	**3**	**4**
Formula	$C_{19}H_{22}GdN_5O_{15}V$	$C_{19}H_{22}N_5O_{15}TbV$	$C_{19}DyH_{22}N_5O_{15}V$	$C_{19}ErH_{22}N_5O_{15}V$
M_r	768.60	770.27	773.85	778.61
Crystal system	Monoclinic, $P2_1/c$	Monoclinic, $P2_1/c$	Monoclinic, $P2_1/c$	Monoclinic, $P2_1/c$
a /Å	15.27250(18)	15.30291(19)	15.0536(3)	15.7195(3)
b / Å	16.9735(2)	16.9273(2)	16.8695(3)	16.4891(3)
c / Å	10.05404(13)	10.05128(12)	9.9480(2)	10.0565(2)
β / °	95.3475(11)	95.0619(12)	96.3710(10)	93.312(2)
V / Å^3	2594.94(6)	2593.50(6)	2510.66(8)	2602.29(9)
Z	4	4	4	4
T / K	293	293	100	293
X-ray wavelength /Å	CuKα	CuKα	AgKα	CuKα
D_c / g cm^{-3}	1.967	1.973	2.047	1.987
μ / mm^{-1}	20.139	17.019	1.814	9.583
F(000)	1512	1516	1520	1528
Reflections collected/unique	14284/4716	13202/4716	44181/5130	15025/4732
Data/restraints/parameters	4716/39/392	4716/39/392	5130/4/399	4732/24/383
Goodness-of-fit (GOF) on F^2	1.045	1.025	1.049	1.088
R_1, wR_2 ($I > 2\sigma(I)$) ^{a,b}	0.0612/0.1627	0.0359/0.0942	0.0214/0.0553	0.0417/0.1078
R_1, wR_2 (all data) ^{a,b}	0.0667/0.1659	0.0381/0.0958	0.0237/0.0560	0.0440/0.1092
CCDC number	2089692	2089693	2089694	2089695

^{a} $R_1 = \sum(|F_o| - |F_c|)/\sum|F_o|$, ^{b} $wR_2 = \{\sum[w(F_o^2 - F_c^2)^2]/\sum[w(F_o^2)^2]\}^{1/2}$

Table S3 Deviations from ideal geometry shapes for Ln^{III} atoms calculated by SHAPE software

Structure [ML10]	**1**	**2**	**3**	**Structure [ML9]**	**4**
Decagon	36.353	36.120	36.099	Enneagon	35.601
Enneagonal pyramid	25.387	25.535	25.022	Octagonal pyramid	22.268
Octagonal bipyramid	16.247	16.373	16.107	Heptagonal bipyramid	17.310
Pentagonal prism	11.574	11.505	11.730	Johnson triangular cupola J3	15.204
Pentagonal antiprism	10.847	10.843	10.634	Capped cube J8	10.188
Bicapped cube J15	9.807	9.716	9.126	Spherical-relaxed capped cube	8.339
Bicapped square antiprism J17	4.995	4.847	4.039	Capped square antiprism J10	2.880
Metabidiminished icosahedron J62	7.737	7.708	7.310	Spherical capped square antiprism	1.631
Augmented tridiminished icosahedron J64	18.845	18.531	18.850	Tricapped trigonal prism J51	4.338
Sphenocorona J87	3.032	2.946	3.019	Spherical tricapped trigonal prism	2.655
Staggered Dodecahedron (2:6:2)	3.510	3.536	3.789	Tridiminished icosahedron J63	11.448
Tetradecahedron (2:6:2)	2.673	2.681	2.909	Hula-hoop	10.344
Hexadecahedron (2:6:2) or (1:4:4:1)	6.851	6.906	6.497	Muffin	1.910

Table S4 Deviations from ideal geometry shapes for V^{IV} atoms calculated by SHAPE software

Structure [ML6]	1	2	3	4
Hexagon	33.213	33.224	33.313	33.240
Pentagonal pyramid	25.613	25.609	25.457	25.580
Octahedron	0.975	0.979	0.996	1.001
Trigonal prism	13.498	13.498	13.345	13.674
Johnson pentagonal pyramid J2	29.546	29.536	29.317	29.434

Table S5 The parameters of O-H···O hydrogen bonds in **1**-**4**.

D–H···A	*d*(D-H)/Å	*d*(H···A)/Å	*d*(D···A)/Å	<(DHA)	Symmetry operation
1					
O3–H3A···O15	0.86	2.08	2.851(9)	148.9	x, y, -1+z
O3–H3B···O9	0.86	2.36	3.186(12)	161.1	1-x, 1-y, -z
O3–H3B···O7	0.86	2.74	3.286(9)	123.4	x, y, z
2					
O3–H3A···O15	0.86	2.07	2.835(5)	148.0	x, y, -1+z
O3–H3B···O9	0.86	2.41	3.236(7)	161.7	1-x, 1-y, -z
O3–H3B···O7	0.86	2.69	3.237(5)	122.9	x, y, z
3					
O3–H3A···O12	0.85	1.97	2.809(3)	169.0	x, y, -1+z
O3–H3B···O9	0.84	2.18	3.014(3)	173.0	1-x, 1-y, -z
4					
O3–H3A···O15	0.95	1.99	2.933(10)	168.9	x, y, -1+z
O3–H3B···O11	0.95	2.35	2.962(9)	121.2	x, y, -1+z
O3–H3B···O9	0.97	2.25	3.075(6)	143.2	x, y, z

Table S6 Fitted parameters derived from DC magnetic data

	2 (Tb) $\lvert J\rangle$	**3** (Dy) $\lvert J\rangle$	**4** (Er) $\lvert J\rangle$	**2** (Tb) $\lvert LS\rangle$	**3** (Dy) $\lvert LS\rangle$	**4** (Er) $\lvert LS\rangle$
J (V-Ln) (cm^{-1})	0.245	-0.254	-0.140	0.775	-0.698	-1.56
g_{xy} (Ln)	1.49	1.28	1.29			
g_z (Ln)	1.46	1.46	0.86			
D (Ln) (cm^{-1})	-6.51	7.45	-1.51	52.2	24.1	98.4
E/*D* (Ln)	0.0326	0.0268	0.248	0.248	0.021	0.007
σ (Ln)				0.949	0.960	0.970

Table S7. The zero-field splitting and g-tensor parameters calculated by OpenMOLCAS/ SINGLE_ANISO for pseudospin *J* of Ln^{III} in compounds **2-4**

|*JM*>	Tb^{III}, *J* = 5	Dy^{III}, *J* = 15/2	Er^{III}, *J* = 15/2
D (cm^{-1})	6.796	4.367	-2.544
E (cm^{-1})	-1.518	0.755	0.458
g_x	1.486	1.328	1.195
g_y	1.491	1.325	1.195
g_z	1.500	1.323	1.194

Table S8 Structures of studied compounds with optimized hydrogen atoms, which were used for theoretical method inputs

Gd	4.23031589380655	8.80421610434115	2.61130519853841
V	2.24729847669359	7.35314954053888	5.09536525677989
O	3.85571410723178	6.92591980300138	4.03478378427166
O	2.79940786795862	9.17079806260417	4.49579585548380
O	5.89165878952986	6.89643482764832	2.43610189119907
O	3.67952750547476	11.21700781409789	3.13984558050621
O	1.05711548389845	7.01197657659352	4.11786707778699
O	3.89542306813103	7.65103560296233	6.69670957126963
H	4.68709344882997	7.91962770656217	6.17829258201702
H	3.72908993608264	8.41791752681752	7.27596298975652
O	5.70750782975520	9.35757722523311	4.55707390078245
O	6.38496003672556	9.91148941654147	2.61338628771168
O	7.62817838429698	10.31201407515425	4.34383561658187
O	5.26246554595326	8.50035404704006	0.19114811184466
O	4.12262098198591	10.19051343818153	0.55228470266220
O	4.75965440758151	9.80933056989127	-1.43599609603835
O	2.99055923984422	7.14096332867978	1.30145893181674
O	1.88538362506313	8.87497879144712	1.78571446030135
O	0.86725073127428	7.17751844279478	0.89329609032408
N	2.26219417917211	5.44516605014039	5.94204308927269
N	1.10698184752592	8.22284456022387	6.59443221692883
N	6.60887634561161	9.86815656715816	3.87506333261989
N	4.72935192682757	9.50008484294589	-0.25524751629093
N	1.88721393416720	7.71479746757967	1.32319022144722
C	2.26278978674067	10.35086943090988	4.77847792517976
C	2.67498093502549	11.48013921311532	4.08173854837297
C	2.15052680837512	12.73329047115247	4.29945232674237
H	2.49270804968889	13.59169314185891	3.71474217614852
C	1.15502396330559	12.88605147858770	5.25714470863404
H	0.71469031085436	13.87687145001610	5.42052392780990
C	0.74036601025270	11.82290364594974	5.99905286332650
H	-0.02944339932608	11.95453078444491	6.77108070234065
C	1.27963857187523	10.53065145379304	5.80225498159399
C	0.80857435448979	9.46569654196301	6.66041860938243
H	0.07352161440832	9.78981972095824	7.42392397110268
C	0.28027660263431	7.25518005045657	7.48667136018126
H	-0.09621922673525	7.84957890939954	8.34170687822052
H	-0.59350480811798	6.96946602598383	6.86863265578614
C	1.01887896550231	6.06329585358766	7.93623017793100
H	1.96973055528148	6.35282074893810	8.42888274021209
H	0.41219100866394	5.60645143051412	8.74506758358992
C	1.23530213210309	5.07174295326698	6.93191915956788
H	0.29798978360047	4.88034589975315	6.36597586472633
H	1.52548028696788	4.09996074348963	7.38082746816493
C	3.02596105256738	4.51610983362299	5.55113566033656
H	2.89533550342618	3.51029608559175	5.99837128149079
C	4.10349548797422	4.57539359814327	4.58560806155949
C	4.81281726321532	3.40343186327933	4.35156758942472
H	4.51146038608323	2.49366217536036	4.88834418307752
C	5.85402349571165	3.36246567390003	3.48105070872763
H	6.39098313639384	2.42288800556874	3.30474436454957

C	6.25091413662334	4.50358240334237	2.81840482832758
H	7.09634395208984	4.47191904286630	2.12411544022592
C	5.57262689761978	5.68062354501146	3.03035515869965
C	4.47706789647701	5.75566782889430	3.87804209231736
C	4.40770203881129	12.36915065794697	2.64558264928736
H	5.23488011777449	11.96687453489540	2.04592618507372
H	4.79438242542688	12.96094228113947	3.49433611017369
H	3.76009259368946	12.98335284611760	1.99646477180323
C	7.25002796077816	7.00200129035281	1.90842014695188
H	7.38381424191964	8.05716583664322	1.63620954300954
H	7.35348630159420	6.38046790138826	1.00320428797841
H	7.97304721281180	6.69876325961725	2.68587117039771

Tb	10.60947042051786	8.13640733843592	2.38405082876606
V	12.58687173887926	9.59674449918716	-0.08240522537432
O	10.96818563792711	10.01205037220605	0.97579696375244
O	12.04347331096572	7.77430761039490	0.52020248117289
O	13.77488081761629	9.95462788955077	0.90344839856378
O	10.93458128411027	9.28582215046200	-1.68355556775034
H	11.10114876117609	8.52700046342021	-2.27324387389638
H	10.15455522863361	9.00014508732195	-1.15516090762408
O	8.93636600928995	10.01825525213805	2.57425148872587
O	11.16504626502937	5.73375338765614	1.86618973051959
O	11.82760145717940	9.78453945451218	3.69710825052842
O	13.95557608301026	9.74364065345853	4.12487954864301
O	12.94203107980828	8.04697370029137	3.21153629229587
O	10.11994982893973	7.15979308635356	6.45447679895697
O	9.55779160187337	8.44722640109629	4.82713510998793
O	8.46685421045309	7.03036914379827	2.38519693121791
O	9.16047622322216	7.60078452745768	0.43546329258335
O	7.23395923218609	6.62398902228983	0.65873428345799
O	10.70769105967172	6.77562205941553	4.42760757996823
N	12.55869799479536	11.49828781918787	-0.92560835664059
N	13.74363730074898	8.72814531120795	-1.58284576746316
N	8.25232374091829	7.06815894446835	1.13116962728093
N	12.94709908992024	9.20634939294280	3.69644914961661
N	10.12556318733224	7.46651453671681	5.27612872494844
C	10.34984064693852	11.18645184557174	1.12168993750443
C	9.25168878697171	11.24132009159437	1.98619513821776
C	8.56538012638195	12.41322076187340	2.20332494724978
H	7.72136421442534	12.43829429223334	2.89953559720608
C	8.95525110156146	13.56751639248204	1.54499832576240
H	8.41163743610460	14.50148845104068	1.73054998723636
C	9.98992958550522	13.53640466446730	0.67163140776792
H	10.29106224654906	14.44594508784914	0.13544601817996
C	10.70873436753029	12.35094025875683	0.43239720973687
C	11.77911113680300	12.43154684683951	-0.53813123316909
H	11.90090247965155	13.43556299736757	-0.98797825644513
C	13.58684941335132	11.88701219510958	-1.91397765262706
H	13.29399889188614	12.85805518852145	-2.36157915157416
H	14.52875787475677	12.06894826331298	-1.35542448173818
C	13.79394926553439	10.87318486012291	-2.94097503825522

H	14.39179662009941	11.32063654120680	-3.75936928179392
H	12.83786462099003	10.56072504197610	-3.40366918994991
C	14.56812994648617	9.67560905388325	-2.43943926300894
H	15.41381550534469	10.00578987973516	-1.80533693632662
H	14.99032166964048	9.09132456808415	-3.28093278984932
C	14.02897907263228	7.48883633305668	-1.63990968905563
H	14.76771586384887	7.15858307131227	-2.39816086317211
C	13.55626309598694	6.42257698140179	-0.78313239092212
C	13.66186405902272	4.06605267038550	-0.25841913210488
H	14.09616170849489	3.07398456458520	-0.43193529996089
C	12.68132407697502	4.21558455342799	0.69796192113080
H	12.33950683814960	3.35326625673787	1.27785942807851
C	12.15455404976351	5.46690120115804	0.92877755297021
C	12.58051635223555	6.59578794058226	0.22430602159525
C	7.58770994190197	9.91533146068190	3.11687785709504
H	6.85538601656681	10.22621324194640	2.35107990592265
H	7.49698170049888	10.53104538997256	4.02751446640196
H	7.45160558412872	8.85936444587548	3.38388565086954
C	10.43302854414510	4.57928888516873	2.37609802621262
H	11.08859703370873	3.96808489322838	3.01922994033004
H	10.03847090177568	3.98797573606949	1.53121175461829
H	9.61510936017361	4.98972891690520	2.98199641646641
C	14.08773810320594	5.13231861203525	-0.99795080978968
H	14.85467319606783	5.00023645947011	-1.77216683304753

Dy	9.82817962583761	8.13119197828618	7.30984530938112
V	11.83217918839269	9.53108473126220	4.84125349456290
C	11.77663776953551	6.54869164276579	5.16316565906655
C	11.33517809158155	5.43336257447515	5.89817219364560
C	11.85969383528148	4.17379302216061	5.70646949424462
H	11.50767840907331	3.32590644144968	6.30107149878074
C	12.86903075384630	3.99139869786682	4.75983909898466
H	13.30741489854448	2.99680907271023	4.61898109795154
C	13.30364081153832	5.05598398810682	4.00698221910849
H	14.08141874221712	4.91157873809076	3.24575539469754
C	12.75780550798398	6.34749275480809	4.17801316540565
C	13.22605287170166	7.38540903344612	3.27971368840816
H	13.96294640384970	7.04205078089739	2.52688090152707
C	13.81798156632948	9.59175662985697	2.47567214208546
H	14.67031435583718	9.86233182558228	3.12725504912770
H	14.21143603797143	9.00444636468932	1.62352659251129
C	13.08659911310343	10.81976593782521	2.01032673441955
H	13.69131185146914	11.25316858043456	1.18803761376271
H	12.11772622603922	10.54793161621253	1.54748717911231
C	12.92332710713639	11.82249070966266	3.03432708774848
H	12.65452179707334	12.80688249243010	2.60194773071979
H	13.87014004314462	11.97133725712544	3.59455429551019
C	11.11430339607168	12.39370122118419	4.39946571115726
H	11.26284063808311	13.39659835982472	3.95537201447543
C	10.02191204019389	12.33125260428426	5.35088672978890
C	9.29180023317513	13.52158438838264	5.54591229805790
H	9.60861863452372	14.42521852282682	5.00918065411792
C	8.21321257598068	13.55931265757517	6.38077748060944

H	7.65912967747111	14.49361314786790	6.52935281442095
C	7.79962147129617	12.40793500568131	7.05042251857141
H	6.92831165860273	12.44437099836852	7.71084209451062
C	8.49909612559017	11.23330674842463	6.87427057541482
C	9.63122087189632	11.17323632141091	6.04222360766149
C	9.61609171884385	4.58525998522468	7.35905297810302
H	9.23544860349587	3.95860032358811	6.53327966867089
H	8.78584062130699	5.00274114923422	7.94285492564814
H	10.27423777576137	4.00520563235430	8.02815067746503
C	6.80424478818182	9.93645073549150	7.95780721872849
H	6.69367314492886	10.56691745934608	8.85619175405568
H	6.65037259216670	8.88684426970462	8.23975821852206
H	6.09546674944825	10.24239173006853	7.16808501437836
N	12.93804901592471	8.63322417091579	3.32752673175395
N	11.88311783720499	11.44463295800977	4.02178420340330
N	7.46160590604274	7.07501054730623	6.10860854565572
N	9.27621494682733	7.47011659895749	10.16362128732239
N	12.16049050202983	9.18088918986665	8.59854456911457
O	11.22316873445755	7.73042207451074	5.43411576088598
O	10.24934119131428	9.99154171543958	5.93000845072385
O	10.20128977355990	9.31220493138461	3.25337913966400
O	13.04818983601155	9.83230780953903	5.82331116066720
O	10.33322351043367	5.72763169845692	6.81597109000383
O	8.16411017322108	10.01902817486349	7.45191021303936
O	8.35940127689335	7.59236704993407	5.39155881115608
O	7.70363380873644	7.03889555363387	7.37173422405762
O	6.41753386171151	6.63821598579704	5.66045985893902
O	9.99181294647297	6.81592153268537	9.34650456203030
O	8.64593586304024	8.44729911806959	9.70759792847742
O	9.21928121698564	7.13505779263971	11.35462344543094
O	10.99990146231621	9.71941158160318	8.69179078131124
O	12.18697583282354	8.04207267674152	8.04427059854779
O	13.15619906978699	9.73637511205781	9.02125719926378
H	10.36404729756046	8.55473700471149	2.66067344167432
H	9.39949361213803	9.04502559188742	3.75699440175707

Er	4.43336607130122	7.81030530400441	2.78047291420480
V	2.43160067202685	9.41904537554727	5.06354386783605
O	4.09327159857136	9.72072569009611	4.03840530113895
O	2.91801135533878	7.57333430125829	4.51722418897326
O	6.07284905579019	9.60087055774205	2.38984628052661
O	3.81092751621486	5.49128056553736	3.26055038348932
O	2.21814088822485	7.58707549526519	1.81983636726380
O	3.32199779563541	9.35709591959302	1.32796446201846
O	5.76581297516685	7.38571289142119	4.77798504620680
O	6.52116073803832	6.68583701121407	2.90861748405090
O	4.96217758853557	6.91807596786917	0.78434445654104
N	2.20441802081907	8.73164537422782	1.27012636974625
N	6.68884440936070	6.79684084565644	4.17466189937863
O	1.28956956332659	9.80525045274262	4.03205029789821
O	4.01821366432477	9.03779753347649	6.69768092470960
N	2.55653026659083	11.33854172176684	5.86187037444465
N	1.17379235796841	8.64265613663941	6.53958005136832

C	4.74618674584100	10.87761136698346	3.82953796509621
C	2.38911383596480	6.41069406262651	4.88267059174854
C	5.81578252479276	10.84537499442285	2.91947200364506
C	7.38120023526442	9.42718292297423	1.78564443400392
C	2.83692128581905	5.25142362446250	4.23006479295079
C	4.48860690083445	4.33960098559747	2.73678337392580
N	4.87206779361766	7.36826082769295	-0.36912593595784
O	1.23441370051335	9.21514616317975	0.73258005056980
O	7.67997496119752	6.39326267896436	4.70766658926515
H	4.79841256174619	8.69496183513507	6.20047226924026
H	3.81107187136024	8.31695849522244	7.32088005902956
C	3.38536645727207	12.21868178475556	5.46227390630246
C	1.53273707173685	11.78307565077784	6.83540836369434
C	0.42300092983968	9.58729741311357	7.40855892466232
C	0.92092129424090	7.39546310858109	6.67700635783851
C	4.42686464529330	12.07176756896354	4.47311273843395
C	1.42345322637486	6.28453556082865	5.90800101120361
C	6.52558440018592	12.00529003600990	2.63951246537146
H	8.16377576320499	9.71832556230401	2.50850177698314
H	7.45120011525118	10.01828301038048	0.85760124173052
H	7.45760234736478	8.36201264204550	1.53082938543679
C	2.32961220954929	4.00627277862449	4.53663873831840
H	5.26323744981049	4.72435411177368	2.05899799152148
H	3.78688968492348	3.70788347374164	2.16343277459015
H	4.95190252085168	3.76059742199853	3.55610939057573
O	5.74836332001179	8.08033843617618	-0.82762908404192
O	3.86972810305150	7.29632355678858	-1.08220637956279
H	3.31833309526229	13.23499826258124	5.89731759944241
H	0.60930168567676	12.00843501166906	6.26319107594014
H	1.86722927204686	12.73094505582865	7.30126228812238
C	1.24459437483268	10.75182593891758	7.88353449495421
H	0.00711715672167	9.02557283315316	8.26880718042083
H	-0.43858754091519	9.95532604210293	6.81453242722780
H	0.19716106638073	7.10107082338154	7.46353460384788
C	5.17610257379407	13.22564371750241	4.17476761210672
C	0.92020713919788	5.00517321787051	6.19372767831727
H	7.34802683339037	11.98327797261541	1.91722009193619
C	6.18823317290737	13.18235453079939	3.26286990948148
C	1.35467736456864	3.89825771384967	5.52338877725651
H	2.67840897060372	3.11362997809947	4.00884760329271
H	0.66862409885810	11.24789613641184	8.68924581592662
H	2.18508426205845	10.40710357871145	8.35557436004418
H	4.92178831872008	14.16610379423142	4.68018050756735
H	0.15802172939104	4.90569408263936	6.97831088328616
H	6.75250338494894	14.09281168530454	3.02689030043618
H	0.93933654840652	2.91203840614738	5.76154032402169

Table S9. The g-values of V^{IV} ions in **2-4** calculated by OpenMOLCAS/SINGLE_ANISO.

Compound	g_x	g_y	g_z	Energy of first excited state (cm^{-1})
2	1.981	1.976	1.930	15495
3	1.981	1.978	1.930	15292
4	1.983	1.981	1.929	15553

Table S10. The splitting of the lowest multiplet for Tb^{III} ion in **2** calculated by OpenMOLCAS/ SINGLE_ANISO together with g-values for selected pseudo-doublets and respective tunneling rates.

E (cm^{-1})	
0.000	g_x = 0.000, g_y = 0.000, g_z = 17.726
0.651	Δ_{tun} = 0.651 cm^{-1}
89.501	g_x = 0.000, g_y = 0.000, g_z = 16.147
93.846	Δ_{tun} = 4.345 cm^{-1}
108.891	
121.934	
163.741	
178.307	
192.549	
257.802	
258.184	
321.839	
322.995	

Table S11. The splitting of the lowest multiplet for Dy^{III} ion in **3** calculated by OpenMOLCAS/ SINGLE_ANISO together with g-values for each Kramers doublets and respective transition magnetic moments within each doublet quantifying probability for the quantum tunneling (QTM).

E (cm^{-1})	g_x	g_y	g_z	QTM
0.000	0.222	0.368	18.941	0.0985
23.392	0.029	0.148	18.007	0.1491
111.912	0.547	0.714	17.573	0.8288
130.534	1.786	3.261	11.982	1.5705
185.411	8.694	5.841	1.911	1.7658
221.276	0.183	1.458	14.732	0.4392
245.258	0.929	3.766	13.144	1.0938
400.088	0.012	0.148	19.018	0.4337

Table S12. The splitting of the lowest multiplet for Er^{III} ion in **4** calculated by OpenMOLCAS/ SINGLE_ANISO together with g-values for each Kramers doublets and respective transition magnetic moments within each doublet quantifying probability for the quantum tunneling (QTM).

E (cm^{-1})	g_x	g_y	g_z	QTM
0.000	1.643	3.634	12.603	0.8796
47.547	7.192	6.243	2.807	1.6710
107.675	0.213	3.121	11.756	0.7747
166.728	0.207	3.055	8.518	1.1241
213.253	1.407	4.060	9.693	2.2595
248.201	0.881	3.191	8.006	1.4929
319.477	0.648	3.192	11.203	1.6391
368.499	1.207	3.615	12.732	1.1355

Table S13 NEVPT2 energy difference ($E(M_{max})$-$E(M_{max}$-2)) between states with different multiplicities, and exchange interaction constants

State	ΔE (**2**)	ΔE (**3**)	ΔE (**4**)	$J_{(Tb-V)}$ (**2**)	$J_{(Dy-V)}$ (**3**)	$J_{(Er-V)}$ (**4**)
1	5.217	6.371	3.035	2.12	1.49	1.52
2	0.317	4.514	0.672	1.50	0.09	0.34
3	1.217	1.514	0.572	0.50	0.35	0.29
4	0.317	6.714	-1.828	2.24	0.09	-0.91
5	0.617	2.914	2.072	0.97	0.18	1.04
6	4.217	2.914	-0.228	0.97	1.20	-0.11
7	-0.183	3.514	-7.128	1.17	-0.05	-3.56
8		1.214	0.272	0.40		0.14
9			1.572			0.79
10			-1.228			-0.61
11			0.872			0.44
12			1.372			0.69
13			0.672			0.34
Avg				1.23	0.48	0.03

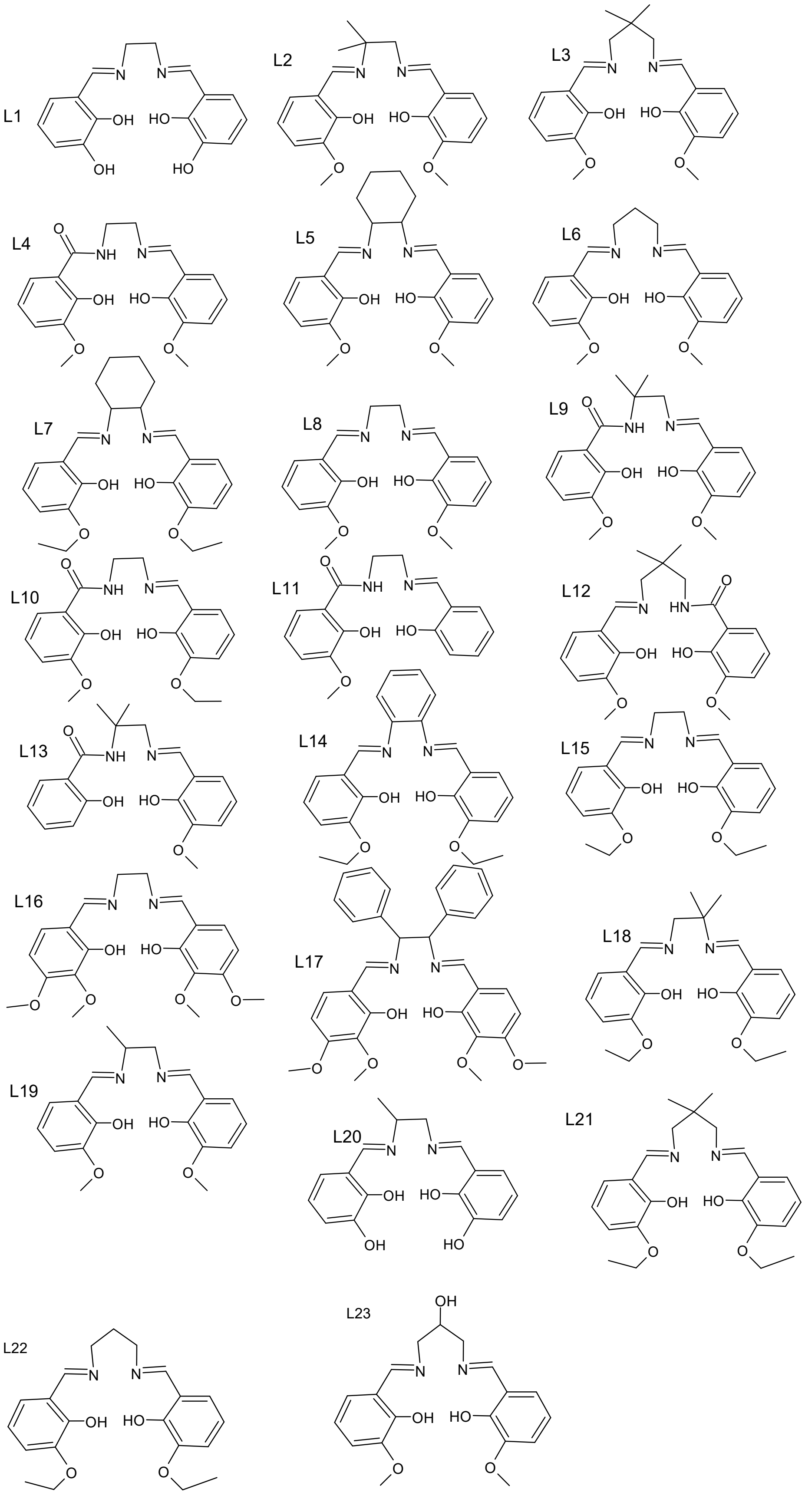

Figure S1: Ligand structures for literature research in Table 1 and Table S1

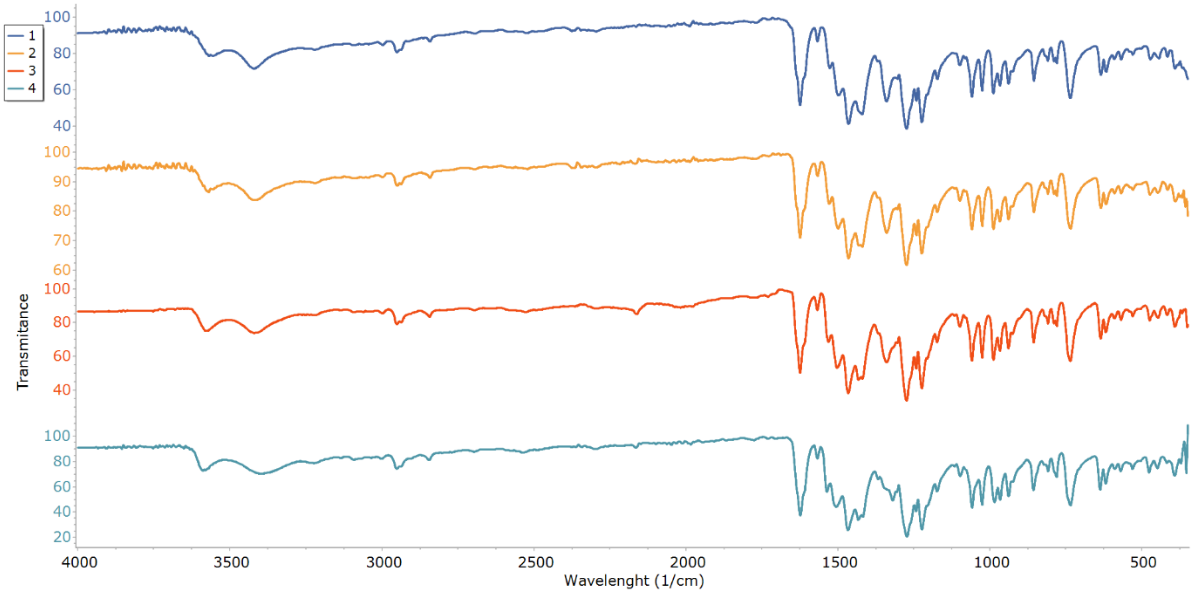

Figure S2 FTIR spectra of prepared compounds

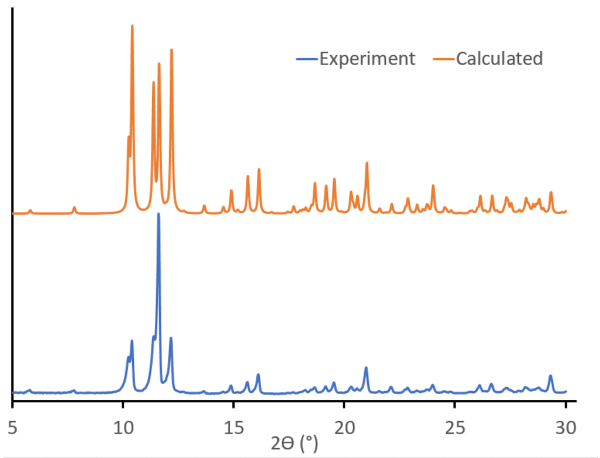

Figure S3 XPD powder pattern of prepared compounds, compared with patterns calculated for structure **1**

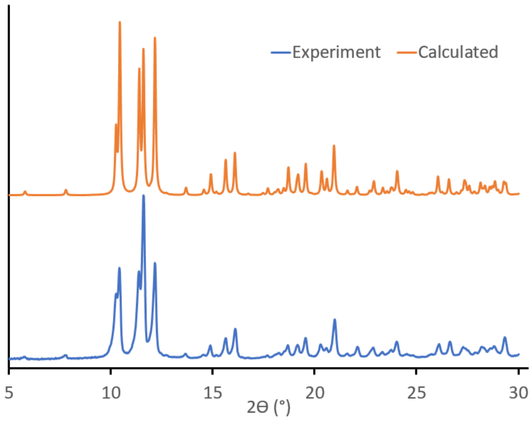

Figure S4 XPD powder pattern of prepared compounds, compared with patterns calculated for structure **2**

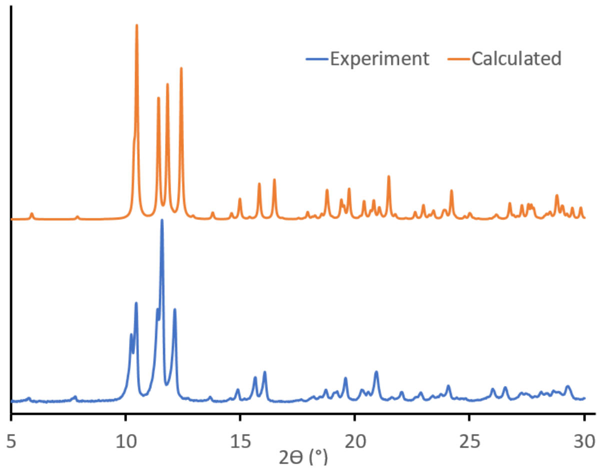

Figure S5 XPD powder pattern of prepared compounds, compared with patterns calculated for structure **3**

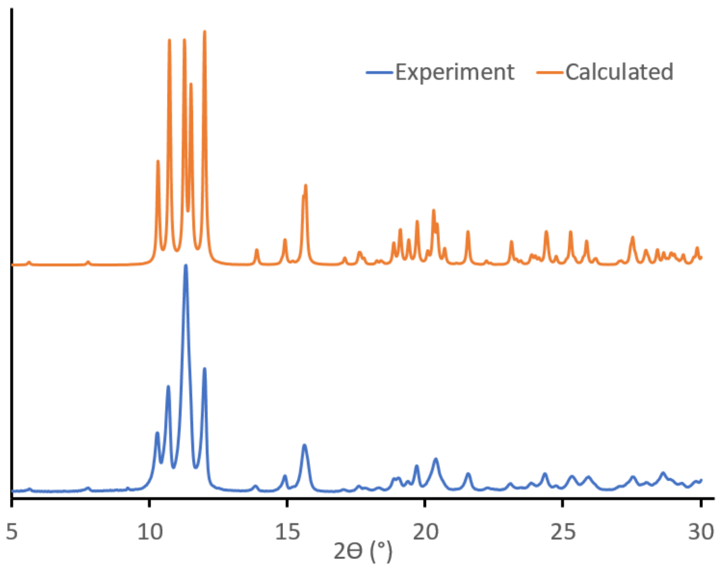

Figure S6 XPD powder pattern of prepared compounds, compared with patterns calculated for structure **4**

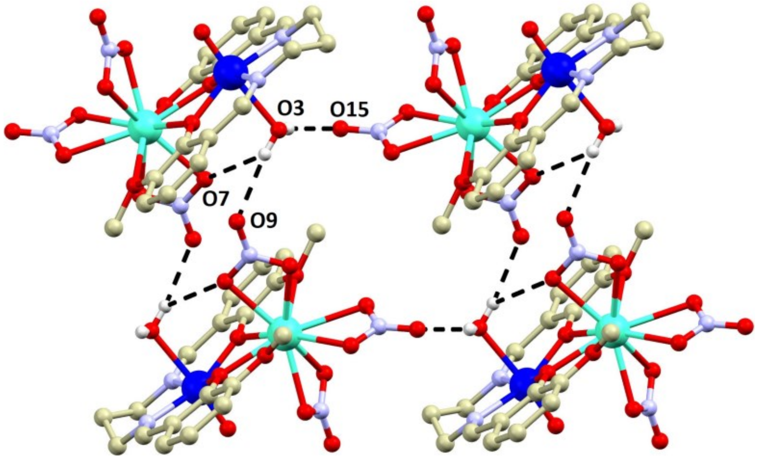

Fig. S7 A perspective view on O-H···O hydrogen bonds (black dashed lines) in **1**.

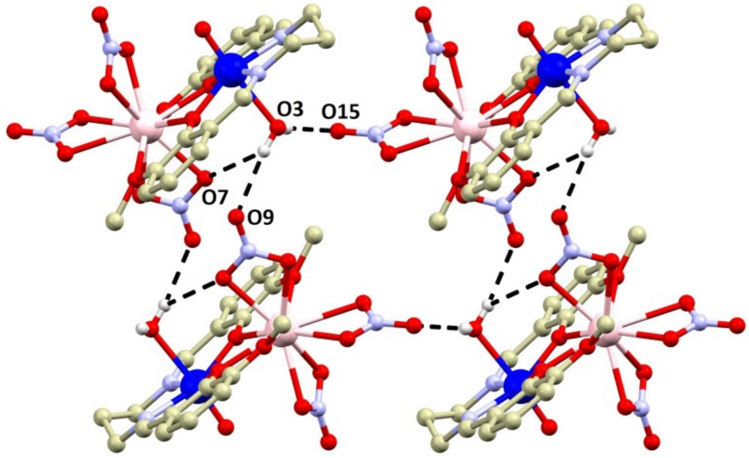

Fig. S8 A perspective view on O-H···O hydrogen bonds (black dashed lines) in **2**.

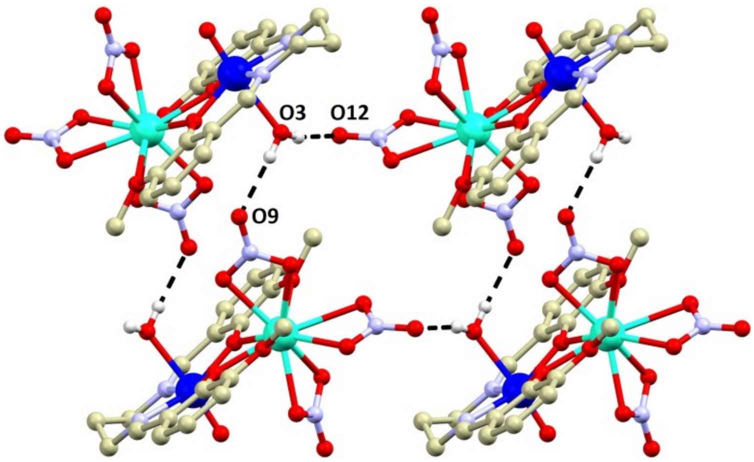

Fig. S9 A perspective view on O-H···O hydrogen bonds (black dashed lines) in **3**.

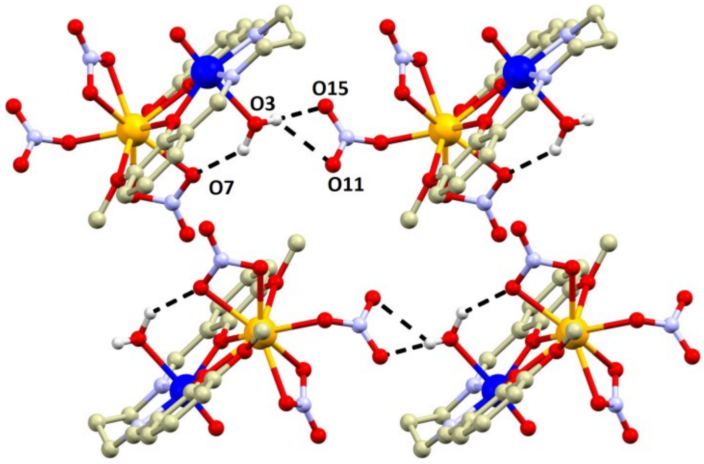

Fig. S10 A perspective view on O-H···O hydrogen bonds (black dashed lines) in **4** (major disorder site).

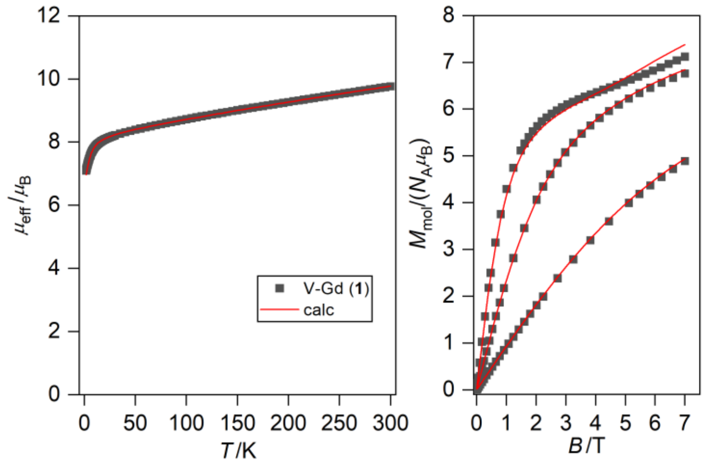

Fig. S11 Magnetic data for **1**. Temperature dependence of the effective magnetic moment μ_{eff} calculated from the mean susceptibility measured at B = 0.2 T and the isothermal magnetizations measured at T = 2, 5 and 10 K. Experimental data – full symbols, calculated data with Eq. 3 and parameters in text – full line.

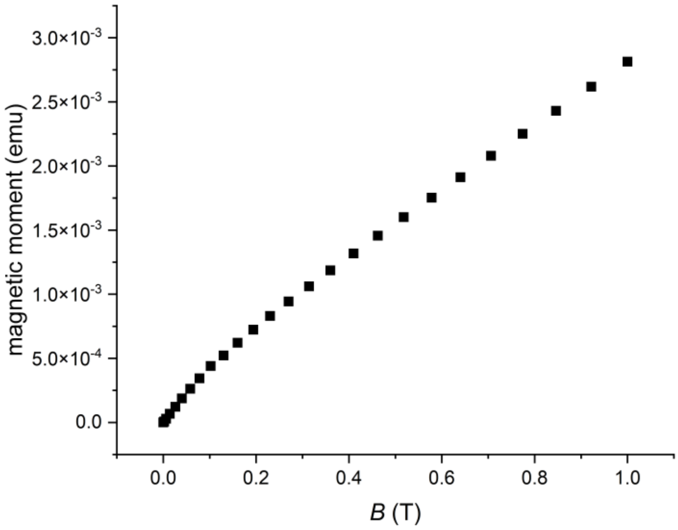

Fig. S12 Magnetic data for **1**. The isothermal magnetic moments measured at T = 300 K.

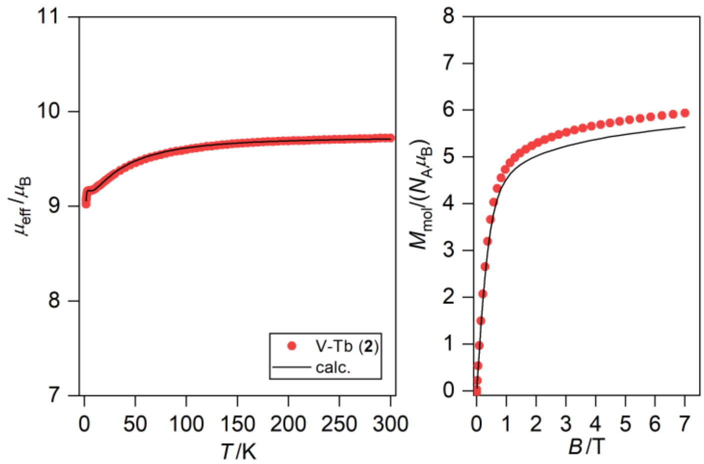

Fig S13 Magnetic data and fit for **2** in JM basis. Temperature dependence of the effective magnetic moment μ_{eff} calculated from the mean susceptibility measured at B = 0.2 T and the isothermal magnetizations measured at T = 2 K. Experimental data – full symbols, calculated data with Eq. 4 and parameters in text – full line.

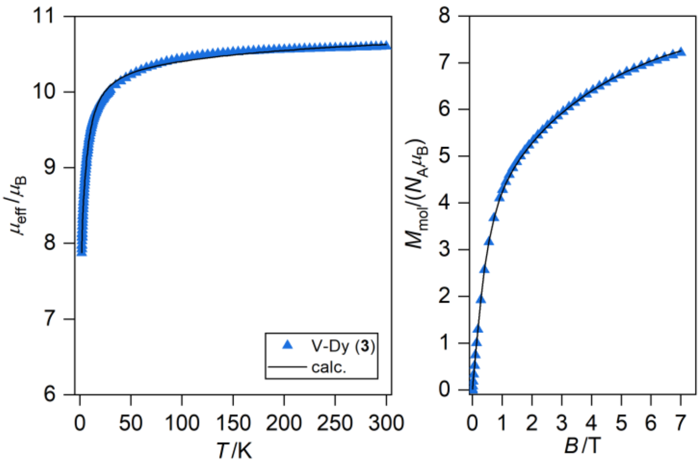

Fig S14 Magnetic data and fit for **3** in JM basis. Temperature dependence of the effective magnetic moment μ_{eff} calculated from the mean susceptibility measured at B = 0.2 T and the isothermal magnetizations measured at T = 2 K. Experimental data – full symbols, calculated data with Eq. 4 and parameters in text – full line.

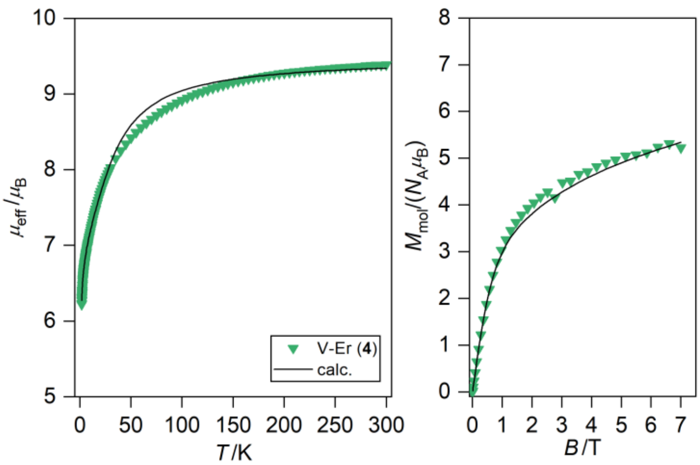

Fig S15 Magnetic data and fit for **4** in JM basis. Temperature dependence of the effective magnetic moment μ_{eff} calculated from the mean susceptibility measured at B = 0.2 T and the isothermal magnetizations measured at T = 2 K. Experimental data – full symbols, calculated data with Eq. 4 and parameters in text – full line.

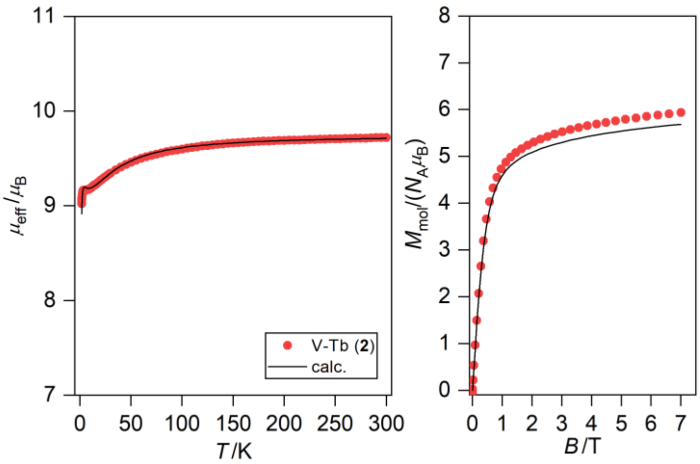

Fig S16 Magnetic data and fit for **2** in LS basis. Temperature dependence of the effective magnetic moment μ_{eff} calculated from the mean susceptibility measured at B = 0.2 T and the isothermal magnetizations measured at T = 2 K. Experimental data – full symbols, calculated data with Eq. 5 and parameters in text – full line.

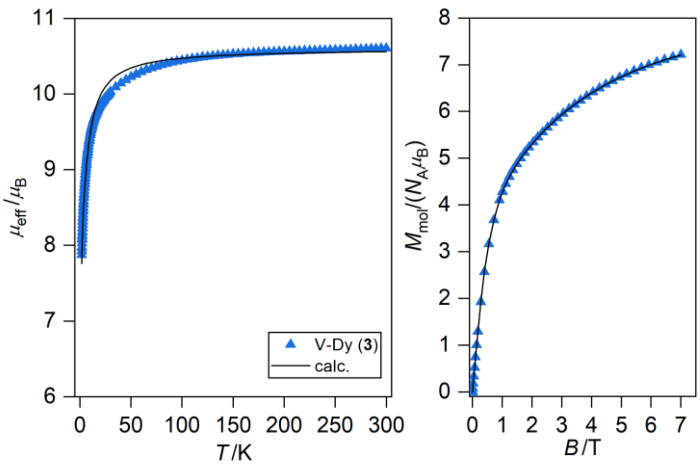

Fig S17 Magnetic data and fit for **3** in LS basis. Temperature dependence of the effective magnetic moment μ_{eff} calculated from the mean susceptibility measured at B = 0.2 T and the isothermal magnetizations measured at T = 2 K. Experimental data – full symbols, calculated data with Eq. 5 and parameters in text – full line.

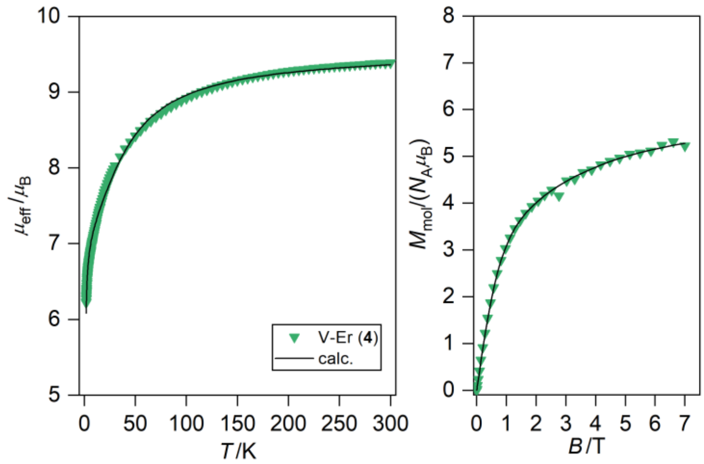

Fig S18 Magnetic data and fit for **4** in LS basis. Temperature dependence of the effective magnetic moment μ_{eff} calculated from the mean susceptibility measured at B = 0.2 T and the isothermal magnetizations measured at T = 2 K. Experimental data – full symbols, calculated data with Eq. 5 and parameters in text – full line.

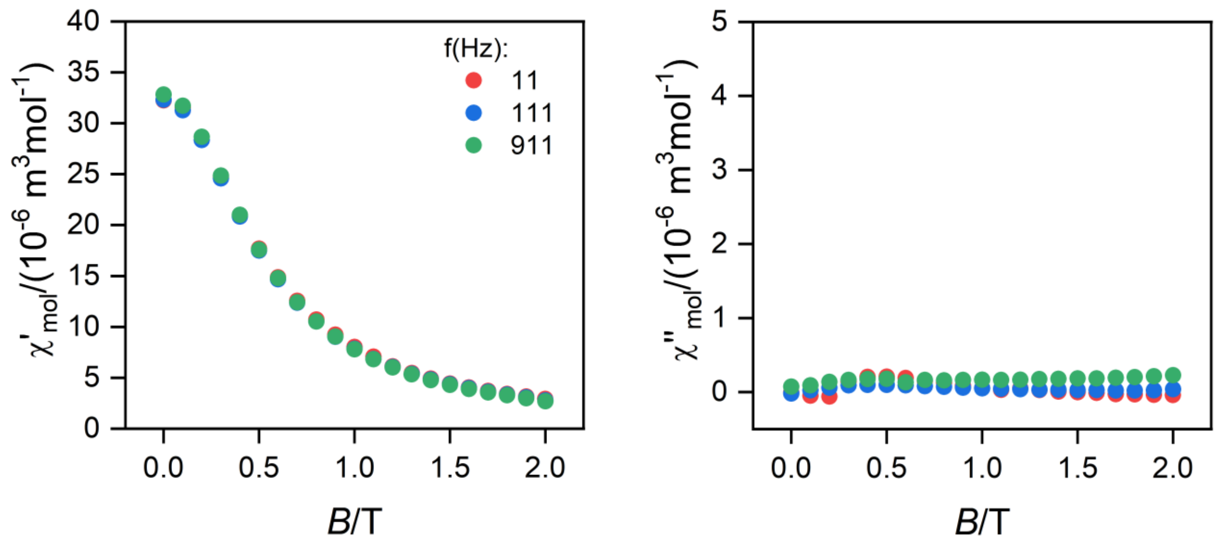

Fig. S19 AC susceptibility data for **4**. The field dependence of real and imaginary molar susceptibilities at T = 2 K.

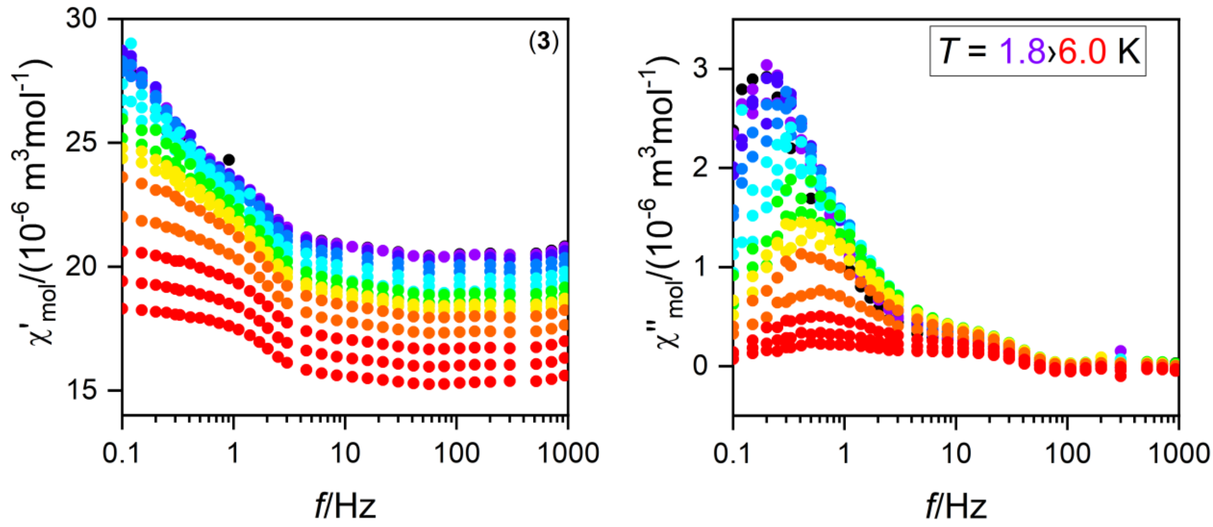

Fig. S20 AC susceptibility data for **3**. The temperature dependence of real and imaginary molar susceptibilities at B = 0.4 T.

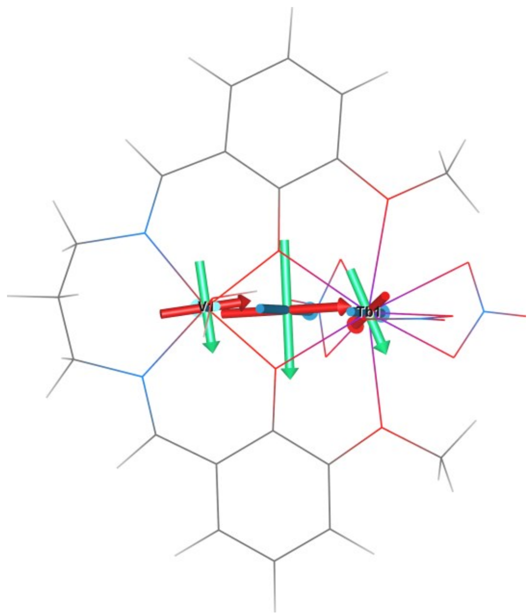

Fig. S21 The molecular structure of **2** derived from the experimental X-ray geometry used for CASSCF calculations overlaid with principal axes of g-tensors of the first Kramers doublet (x/y/z-axes colored as red/green/blue arrows) of V^{IV} and Tb^{III}. The molecular g-tensor axes of the ground state resulting from POLY_ANISO are located in the midpoint of metal atoms and are plotted with longer arrows.

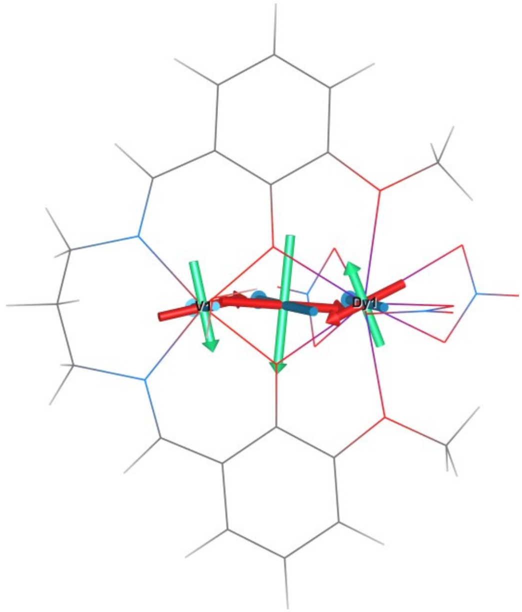

Fig. S22 The molecular structure of **3** derived from the experimental X-ray geometry used for CASSCF calculations overlaid with principal axis of g-tensors of the first Kramers doublet (x/y/z-axes colored as red/green/blue arrows) of V^{IV} and Dy^{III}. The molecular g-tensor axes of the ground state resulting from POLY_ANISO are located in the midpoint of metal atoms and are plotted with longer arrows.

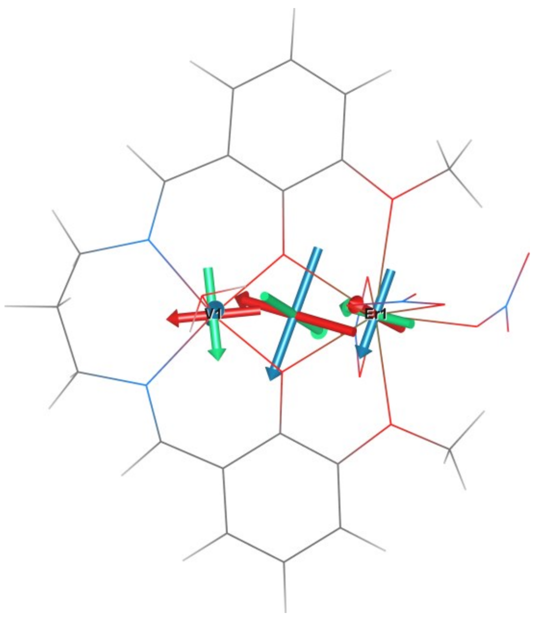

Fig. S23 The molecular structure of **4** derived from the experimental X-ray geometry used for CASSCF calculations overlaid with principal axis of g-tensors of the first Kramers doublet (x/y/z-axes colored as red/green/blue arrows) of V^{IV} and Er^{III}. The molecular g-tensor axes of the ground state resulting from POLY_ANISO are located in the midpoint of metal atoms and are plotted with longer arrows.

Compound **2**	$J_{V\text{-}Tb}$ = +0.716 cm^{-1} Scaling factor for calculated data: 0.985
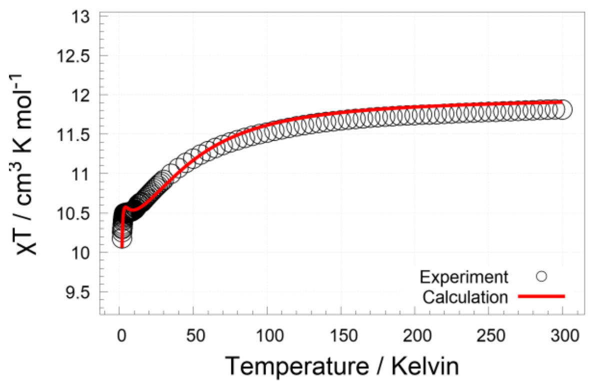	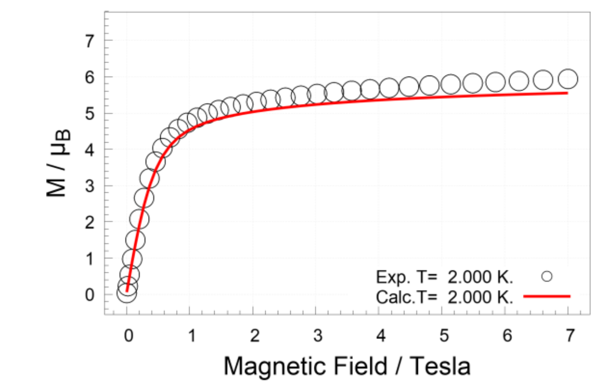
Compound **3**	$J_{V\text{-}Dy}$ = -1.69 cm^{-1} Scaling factor for calculated data: 0.988
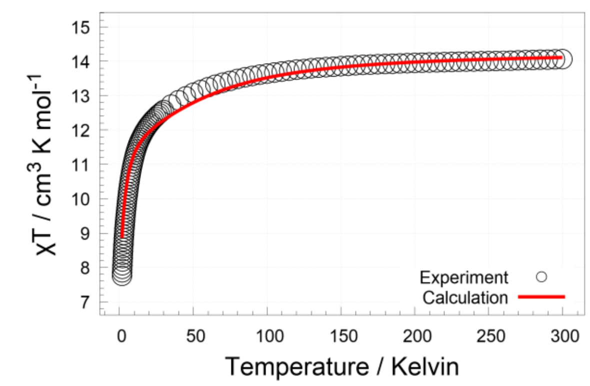	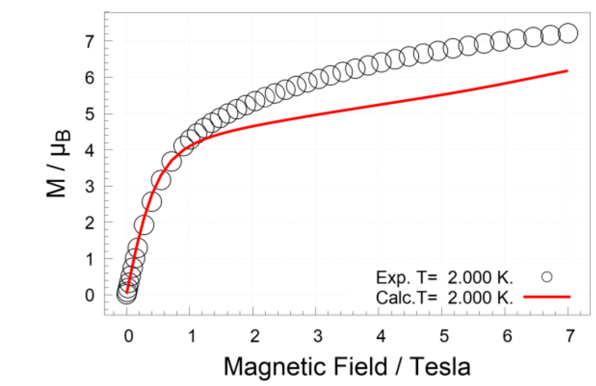
Compound **4**	$J_{V\text{-}Er}$ = -0.736 cm^{-1} Scaling factor for calculated data: 0.932
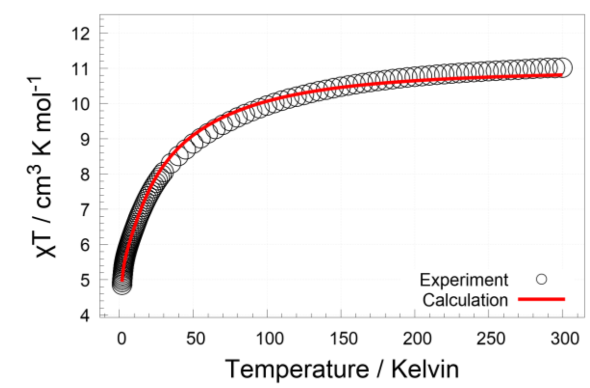	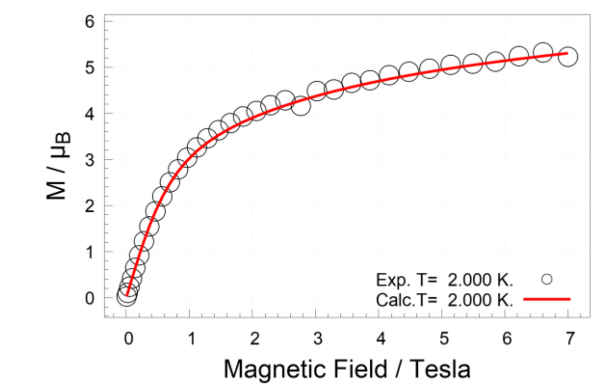

Fig. S24 The best-fits of experimental magnetic data (temperature dependence of mean susceptibility measured at B = 0.2 T and the isothermal molar magnetization measured at T = 2 K) of **2-5** utilizing POLY_ANISO module.

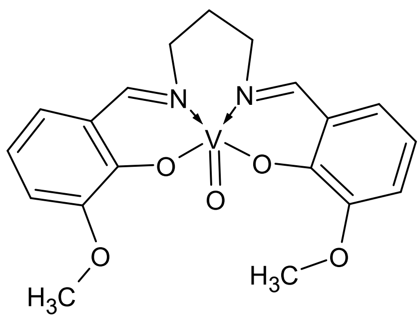

Scheme 1: Expected structure of intermediate product [(VO)L]

Additional literature:

[1] Y.-A. Liu, C.-Y. Wang, M. Zhang and X.-Q. Song, *Polyhedron*, 2017, **127**, 278–286.
[2] H.-R. Wen, J. Bao, S.-J. Liu, C.-M. Liu, C.-W. Zhang and Y.-Z. Tang, *Dalt. Trans.*, 2015, **44**, 11191–11201.
[3] P. Zhang, L. Zhang, S.-Y. Lin and J. Tang, *Inorg. Chem.*, 2013, **52**, 6595–6602.
[4] L. Xu, Q. Zhang, G. Hou, P. Chen, G. Li, D. M. Pajerowski and C. L. Dennis, *Polyhedron*, 2013, **52**, 91–95.
[5] Y. Sui, D.-S. Liu, R.-H. Hu and J.-G. Huang, *Inorganica Chim. Acta*, 2013, **395**, 225–229.
[6] J.-P. Costes, B. Donnadieu, R. Gheorghe, G. Novitchi, J.-P. Tuchagues and L. Vendier, *Eur. J. Inorg. Chem.*, 2008, **2008**, 5235–5244.
[7] J.-P. Costes, M. Auchel, F. Dahan, V. Peyrou, S. Shova and W. Wernsdorfer, *Inorg. Chem.*, 2006, **45**, 1924–1934.
[8] R. Koner, G.-H. Lee, Y. Wang, H.-H. Wei and S. Mohanta, *Eur. J. Inorg. Chem.*, 2005, **2005**, 1500–1505.
[9] R. Koner, H.-H. Lin, H.-H. Wei and S. Mohanta, *Inorg. Chem.*, 2005, **44**, 3524–3536..
[10] O. Margeat, P. G. Lacroix, J. P. Costes, B. Donnadieu, C. Lepetit and K. Nakatani, *Inorg. Chem.*, 2004, **43**, 4743–4750.
[11] G. Novitchi, S. Shova, A. Caneschi, J.-P. Costes, M. Gdaniec and N. Stanica, *Dalt. Trans.*, 2004, 1194–1200.
[12] H. Kara, Y. Elerman and K. Prout, *Zeitschrift für Naturforsch. B*, 2000, **55**, 1131–1136.
[13] J.-P. Costes, F. Dahan and A. Dupuis, *Inorg. Chem.*, 2000, **39**, 165–168.
[14] M. Sakamoto, M. Hashimura, K. Matsuki, N. Matsumoto, K. Inoue and H. Okawa, *Bull. Chem. Soc. Jpn.*, 1991, **64**, 3639–3641.
[15] T. Ishida, R. Watanabe, K. Fujiwara, A. Okazawa, N. Kojima, G. Tanaka, S. Yoshii and H. Nojiri, *Dalt. Trans.*, 2012, **41**, 13609.
[16] L. M. Lilley, K. Du, M. D. Krzyaniak, G. Parigi, C. Luchinat, T. D. Harris and T. J. Meade, *Inorg. Chem.*, 2018, **57**, 5810–5819..
[17] M. Towatari, K. Nishi, T. Fujinami, N. Matsumoto, Y. Sunatsuki, M. Kojima, N. Mochida, T. Ishida, N. Re and J. Mrozinski, *Inorg. Chem.*, 2013, **52**, 6160–6178.
[18] T. Kajiwara, M. Nakano, K. Takahashi, S. Takaishi and M. Yamashita, *Chem. - A Eur. J.*, 2011, **17**, 196–205.
[19] G. Novitchi, J.-P. Costes and B. Donnadieu, *Eur. J. Inorg. Chem.*, 2004, **2004**, 1808–1812.
[20] F. Z. Chiboub Fellah, S. Boulefred, A. Chiboub Fellah, B. El Rez, C. Duhayon and J.-P. Sutter, *Inorganica Chim. Acta*, 2016, **439**, 24–29.